

Characterization of the eyespot and hematochrome-like granules of *Euglena gracilis* by scan-free absorbance spectral imaging $A(x, y, \lambda)$ for quantification of carotenoids within the live cells

Kyohei Yamashita¹, Takafumi Yagi¹, Takumi Isono¹, Yusuke Nishiyama¹, Masafumi Hashimoto¹, Koji Yamada², Kengo Suzuki², Eiji Tokunaga^{Corresp. 1}

¹ Department of Physics, Faculty of Science, Tokyo University of Science, Tokyo, Japan

² Euglena Co., Ltd., Yokohama, Japan

Corresponding Author: Eiji Tokunaga
Email address: eiji@rs.kagu.tus.ac.jp

Euglena gracilis is an edible photosynthetic single-cell alga that can synthesize carotenoids. It is highly demanded to establish the technology to select and grow individual cells capable of synthesizing more carotenoids because it contributes to safe and inexpensive production of carotenoids. In the cells of *E. gracilis*, carotenoids are mainly contained in chloroplasts and eyespots, and typical carotenoids have a characteristic absorption maximum in common. *E. gracilis* also has an organelle resembling hematochrome, which has an appearance similar to the eyespot and the absorption band spectrally overlapping that of the carotenoid although reportedly it does not contain carotenoids. To discriminate the eyespot and hematochrome-like granules and to investigate the intracellular distribution of carotenoids, scan-free, non-invasive, absorbance spectral imaging $A(x, y, \lambda)$ microscopy of single live cells was applied. It was demonstrated that this technique is a powerful tool not only for basic research on intracellular structural analysis but also for identifying difference in carotenoid content in individual cells applicable to screening of carotenoid-rich cells. By this technique, it was confirmed that carotenoids exist in chloroplasts and eyespots, and a number of characteristic absorption spectra of pigments observed specific to the eyespot or hematochrome-like granules were identified. In addition, it was found that hematochrome-like granules have a characteristic absorption peak at 620 nm as well as at 676 nm, suggesting that its origin is a component of chloroplast including Chlorophyll *a*.

1 Characterization of the Eyespot and Hematochrome-like 2 Granules of *Euglena gracilis* by Scan-Free Absorbance 3 Spectral Imaging $A(x, y, \lambda)$ for Quantification of Carotenoids 4 within the Live Cells

5 Kyohei Yamashita¹, Takafumi Yagi¹, Takumi Isono¹, Yusuke Nishiyama¹, Masafumi Hashimoto¹,
6 Koji Yamada², Kengo Suzuki² and Eiji Tokunaga¹

7 Kyohei Yamashita¹, Takafumi Yagi¹, Takumi Isono¹, Yusuke Nishiyama¹, Masafumi Hashimoto¹,
8 Koji Yamada², Kengo Suzuki² and Eiji Tokunaga¹

9 ¹ Department of Physics, Faculty of Science, Tokyo University of Science, Shinjuku-ku, Tokyo, Japan

10 ² euglena Co., Ltd., Yokohama-shi, Kanagawa, Japan

11

12 Corresponding author:

13 **Eiji Tokunaga¹**

14 1-3 Kagurazaka, Shinjuku-ku, Tokyo, 162-8601, Japan

15 eiji@rs.kagu.tus.ac.jp

16

17 Abstract

18 *Euglena gracilis* is an edible photosynthetic single-cell alga that can synthesize carotenoids. It
19 is highly demanded to establish the technology to select and grow individual cells capable of
20 synthesizing more carotenoids because it contributes to safe and inexpensive production of
21 carotenoids. In the cells of *E. gracilis*, carotenoids are mainly contained in chloroplasts and
22 eyespots, and typical carotenoids have a characteristic absorption maximum in common. *E. gracilis*
23 also has an organelle resembling hematochrome, which has an appearance similar to the eyespot
24 and the absorption band spectrally overlapping that of the carotenoid although reportedly it does
25 not contain carotenoids. To discriminate the eyespot and hematochrome-like granules and to
26 investigate the intracellular distribution of carotenoids, scan-free, non-invasive, absorbance
27 spectral imaging $A(x, y, \lambda)$ microscopy of single live cells was applied. It was demonstrated that
28 this technique is a powerful tool not only for basic research on intracellular structural analysis but
29 also for identifying difference in carotenoid content in individual cells applicable to screening of
30 carotenoid-rich cells. By this technique, it was confirmed that carotenoids exist in chloroplasts and
31 eyespots, and a number of characteristic absorption spectra of pigments observed specific to the
32 eyespot or hematochrome-like granules were identified. In addition, it was found that
33 hematochrome-like granules have a characteristic absorption peak at 620 nm as well as at 676 nm,
34 suggesting that its origin is a component of chloroplast including Chlorophyll *a*.

35 **Keywords:** *Euglena*; carotenoid; eyespot; hematochrome; chloroplast; absorbance spectral
36 imaging; photosynthesis; alga; microscopy;

37

38 Introduction

39 *E. gracilis* is a photosynthetic unicellular flagellate microorganism with a length of
40 approximately 50 μm and a diameter of 8 to 12 μm inhabiting freshwater (Jerome, 2012).
41 Depending on nutritional and environmental conditions, *E. gracilis* synthesizes paramylon, a β -
42 1,3-glucan in a crystalline form, which is used as an ingredient of functional food (Sugiyama *et al.*,

43 2009) or produce wax ester suited for its conversion to biofuel (Inui *et al.*, 1982). *E. gracilis* can
44 grow in heterotrophic culture (Koren-Hutner medium (Koren & Hutner, 1967)). Also, since the
45 cells contain about 10 chloroplasts (Yamaji, 1980), they can photosynthetically grow in autotrophic
46 culture (Cramer-Myers medium (Cramer & Myers, 1952)). The success of mass-cultivation of *E.*
47 *gracilis* has realized the commercial supply of *E. gracilis* as an ingredient of functional foods,
48 cosmetics, and biofuel (Suzuki, 2017). Therefore, technology using *E. gracilis*, which enables clean,
49 sustainable, and cost-effective production of energy and food, attracts attention in industrial and
50 academic fields (Yamada *et al.*, 2016).

51 We focus on carotenoid production capacity among many useful properties of *Euglena*. *E.*
52 *gracilis* is one of the few microorganisms capable of simultaneously producing antioxidant
53 vitamins such as β -carotene and vitamin C (Takeyama *et al.*, 1997; Kato *et al.*, 2017). Carotenoids
54 have been used as a coloring and antioxidant for foods from long ago as represented by β -carotene
55 (Gordon & Bauernfeind, 1982; Hardeep *et al.*, 2015; Takaichi, Mimuro & Tomita, 2006). Certain
56 carotenoids also have the potential to reduce the risk of cancers and eye diseases (Johnson, 2002).
57 Therefore, it is also used as a health supplement and an antioxidant from demand due to recent
58 health boom (Joanna & Květoslava, 2014). It is also used as a feed additive for animals (Delia &
59 Rodriguez-Amaya, 2015), and also for an active ingredient of cosmetics (Maxim *et al.*, 2011).
60 Therefore, a mass production method of carotenoids which is inexpensive and guaranteed safety is
61 a task.

62 Carotenoids are synthesized by photosynthetic organisms including algae and play important
63 roles in photosynthesis (constituents of light harvesting pigment-protein complexes) and photo
64 protection (non-photochemical quenching, xanthophyll cycle, etc.) (Barbara, 1990; Havaux, 1998;
65 Hashimoto, Uragami & Cogdell, 2016). Also, most flagellate green algae exhibiting photo
66 responses have a photoreceptive organelle, eyespot. With the eyespot, they can detect the direction
67 of light source in the environment where they are located (Ozasa *et al.*, 2014). It is known that the
68 constituent components of this eyespot are various carotenoids (Merete *et al.*, 1994). The eyespot
69 of *E. gracilis* is an orange-red colored distinct structure with a cross section of $2 \times 3 \mu\text{m}^2$, located
70 near the front end of the cell with flagella. This organelle is composed of the aggregation of a large
71 number of granules (40 to 50) containing carotenoids with a diameter of 0.1 to 0.3 μm in the
72 cytoplasm directly beneath the cell membrane constituting the boundary of the front end
73 invagination called reservoir (Mineo, 2007; Jerome, 2012; Jerome, 2013). (This area is sometimes
74 referred to as stigma. In this paper it is described as eyespot.) Thus, the carotenoid molecules in
75 cells show specific intracellular localization. In order for *Euglena* to receive a modulated light
76 signal during helical swimming, it is believed that the eyespot of *Euglena* is not itself a
77 photoreceptor, unlike many other algae like *Chlamydomonas* (Steven & Shigeoka, 2017), but it
78 plays a role in casting a shadow on photoreceptor (PAB:paraxonemal body) (Mineo, 2007; Barsanti
79 *et al.*, 2009; Georg, 2009).

80 To improve the value of *E. gracilis* for industrial application, breeding methods for this species
81 are established (Yamada *et al.*, 2016a; Yamada *et al.*, 2016b). Fe-ion beam irradiation efficiently
82 induces random mutations and produces a population including various phenotypes of mutants
83 (Yamada *et al.*, 2016b). In addition, efficient selective breeding of oil-rich *E. gracilis* strain is
84 demonstrated by isolating the desired cells from the mutant pool by using fluorescence-activated
85 cell sorting (Yamada *et al.*, 2016a). To accomplish selective breeding of carotenoid-rich *E. gracilis*,
86 methods to measure the amount and type of carotenoids in individual cells are required. Since the
87 aforementioned selective breeding method does not use gene recombination technology, the
88 produced strains can be easily applicable in the industrial production process.

89 Conventional chemical measurement methods require a large number of cells to quantify the
90 carotenoid content. Although there is a method of fluorescently staining substances in cells and
91 observing them with a microscope, there is a concern that the staining themselves may affect cells
92 (*Wojcik & Dobrucki, 2008*). Thus, non-invasive microspectrophotometry is a candidate method to
93 solve the above problem (*Benedetti et al., 1976; James et al., 1992; Valter et al., 2007*). In recent
94 years, a microscopic technique using stimulated Raman scattering (SRS) has been developed as a
95 fast and unstained cell measurement technique. This made it possible to visualize lipids, paramylon,
96 chlorophyll, and proteins contained in *E. gracilis* in a label-free and living state (*Iwata et al.,*
97 *2017*). In their approach, however, carotenoids are not imaged because the number of spectral
98 points is reduced to four characteristic colors between 2,800 and 3,100 cm^{-1} to increase the frame
99 rate of imaging, although Raman imaging of carotenoids is potentially feasible when the imaging
100 rate and a plurality of types of imaged molecules are not so stringent requirement (*Wakisaka et al.,*
101 *2016*). For label-free multicolor imaging of plural types of constituent molecules including
102 carotenoids, therefore, it is desired to explore other approaches than SRS as well. One of the
103 promising approaches is the absorption imaging. Recently, various methods of fast spatial imaging
104 of the absorption spectra $A(x, y, \lambda)$, a three-dimensional (3-D) dataset typically called a datacube,
105 are developed (*Matsuoka., 2002; Kester et al., 2011; Hagen et al., 2012; Lee et al., 2012; Hagen*
106 *& Kudenov., 2013*).

107 In the present research, we have adopted a non-scanning (snapshot) absorption imaging method
108 for imaging of carotenoids which uses a fiber array (2D-1D fiber bundled array) that converts a
109 two - dimensional (16 pixel \times 16 pixel, 0.96 mm \times 0.96 mm) image into a one - dimensional (256
110 pixels, 0.06 mm \times 15.36 mm) image fitted to a spectrometer slit. This method is characterized by
111 obtaining spatially resolved absorption spectral image $A(x, y, \lambda)$ of living cells for an extremely
112 short time (~ 0.05 sec) and with high spatial resolution (about 1 μm). If we can quantify the
113 carotenoids contained in individual cells from the absorption image of the whole one cell, we will
114 be able to efficiently select competent cells.

115 As a preparatory stage, it is necessary to confirm that the distribution of various pigments present
116 in cells and organelles can be discriminately observed. To test this, we focused on chloroplasts,
117 eyespot and hematochrome, as these intracellular structures are reported to contain carotenoids
118 (*Britton & Goodwin, 2013*). Hematochrome has an appearance resembling an eyespot and is known
119 to be a plastid found in red *Euglena*, such as *Euglena sanguinea*, which changes from green to red
120 when irradiated with intense light. It is reported that granules similar to hematochrome are also
121 observed in *E. gracilis* (*STROTHER & WOLKEN, 1961; Dennis, 1982*), and we will refer to it in
122 this paper as hematochrome. The hematochromes appear in *E. gracilis* cells in old culture (*Jerome,*
123 *2012*) and is suggested not to include carotenoids (*Britton & Goodwin, 2013*). Since hematochrome
124 was also found in the mutant that cannot synthesize carotenoid and the cell cultured in a medium
125 to which the carotenoid synthesis inhibitor was added, its origin is considered to be different from
126 that of an eyespot, but details are unknown (*Britton & Goodwin, 2013*).

127 In this paper, absorption spectra inside and around these intracellular structures are measured to
128 be compared and examined using the non-invasive and high spatial resolution absorption imaging
129 method.

130 **Experimental Methods**

131 ***1. Sample Preparation***

132 The wild type *E. gracilis* (Z strain) was cultured in CM medium (Cramer-Myers medium
133 (*Cramer & Myers, 1952*), pH 3.5) for 4 weeks. Cells were kept aerobically under continuous
134 illumination (cool white fluorescent light : 40 [$\mu\text{mol} / \text{m}^2 / \text{sec}$]) and constant temperature (26°C).
135 Cells were harvested by centrifugation (6000 rpm, 5 min, 4°C), then washed with purified water
136 twice and re-suspended in purified water. This suspension of 1mL was added to 5 mL of fresh CM
137 medium (total 6 mL). The initial cell density at this time is 1.2×10^6 [cell / mL]. This culture was
138 kept in the glass tube with the cap sealed for 3 days under continuous illumination (cool white
139 fluorescent light : 100 [$\mu\text{mol} / \text{m}^2 / \text{sec}$]) and constant temperature (26°C).

140 **2. Measurement Methods**

141 Detailed methods of scan-free absorbance spectral imaging are described in Ref. (*Isono et al.,*
142 *2015*). Here, we made the major improvement as follows:

143 Previously (*Isono et al., 2015*), we introduced a fiber bundled array to convert a 2-dimensional
144 image to the 1-dimensional slit image. A 50- μm core/55- μm clad/60- μm coating silica fibers are
145 assembled to 16 \times 16 (0.96 \times 0.96 mm²) array on the input side and to 1 \times 256 (0.06 \times 15.36 mm²)
146 array on the output (slit) side. On the side port of the microscope, the \times 100 magnified image of the
147 sample was focused on the 16 \times 16 2D array ($x \times y$), which is rearranged in order into the 1D array
148 to fit the entrance slit of the spectrometer. Thus, in principle, 256 spectra can be simultaneously
149 obtained on a charge-coupled device (CCD) camera through the spectrometer for a single exposure
150 time. Previously, however, the vertical CCD size was only 6.4 mm such that three or four times
151 measurement is needed by shifting the 1D-array on the slit vertically.

152 In this paper, we have realized scan-free (snapshot) absorbance spectral imaging in the true sense
153 of the word, by replacing both spectrometer and CCD as follows. An imaging spectrometer
154 (MS3504i or SL100M, SOLAR TII) was replaced by that with a larger imaging area of 27 \times 27
155 mm² (f=32 cm, IsoPlaneSCT-Advance, Roper Scientific). An electrically-cooled EM-CCD camera
156 (1600 \times 400 pixels with 16 μm pixel size, DU971N-UVB, Newton, Andor) was replaced by an
157 electrically-cooled CCD camera (2048 \times 2048 pixels with 13.5 μm pixel size, PIXIS2048BUV,
158 Roper Scientific). The vertical size of both the imaging area (27mm) and the CCD (27.65mm)
159 covers that (15.36 mm) of the 1D array of the 2D-1D converter, so that the whole 3D image $A(x,$
160 $y, \lambda)$, a datacube of 16 \times 16 \times 2048, is obtained simultaneously without need for the vertical scan. To
161 be precise, the vertical length in the imaging area where an aberration-corrected image is obtained
162 is limited by 14 mm, so that the images from 22-23 fibers at both ends of the 1D array are not
163 aberration-free. The shortest acquisition time is 0.05 second which is limited by the response time
164 of the mechanical shutter of the spectrometer.

165 A medium diluted to the appropriate cell concentration for observation with purified water was
166 covered with a cover glass on the glass bottom dish (Matsunami glass D11130H). The sample was
167 set on an inverted microscope (IX71, OLYMPUS) and observed with a \times 100 objective lens of NA
168 0.85 from below. The light source was a 150 W Xenon lamp (Hamamatsu) to illuminate a region
169 of 2 mm in diameter of the sample from above through a condenser. The intensity (photon flux
170 density) on the sample was 3450 $\mu\text{mol} / \text{m}^2 / \text{sec}$ for 0.5 second exposure. The transmitted light was
171 transferred through the objective and a focusing lens to the side port of the microscope. The
172 absorbance of the sample was calculated assuming that the transmitted light intensity in the region
173 where only the culture solution exists is 100%. The spectrometer has automatically exchangeable
174 three gratings, 1200, 300, and 150 grooves / 300 nm blaze. We used the 150 grooves grating with
175 wavelength resolution of 1.1 nm at 546 nm (50 μm slit width, determined by the core size of the

176 fiber) and wavelength span from 390 to 790 nm. All the measurements were performed at room
177 temperature.

178

179 **Results**

180 We observed the microscope images of more than 100 cells, among which we selected a
181 specific cell which was slow in movement and where the eyespot and a hematochrome-like
182 granule (we call this hematochrome hereafter) were accidentally located close to each other and
183 not overlapped with a chloroplast. Figure 1 shows a bright-field microscopic image of that cell
184 and Figure 2 shows the absorbance spectral images $A(x,y,488\text{ nm})$ of the eyespot and
185 hematochrome in the enlarged view. Figures 3 and 4 show the local absorbance spectra of the
186 eyespot and hematochrome at the positions labeled in Figs. 2(b) and 2(c), respectively.

187

188 **1. Absorption Image at the Wavelength of the Maximum Absorbance of Carotenoids (Figure** 189 **2)**

190 The data show that absorption is found in hematochrome, chloroplast and eyespot regions in
191 the absorption image at the carotenoid absorbance maximum wavelength 488 nm. Although
192 hematochrome of *E. gracilis* does not contain carotenoids, absorption at this wavelength is large.
193 Therefore, it was suggested that it may be an error factor for imaging the distribution of
194 carotenoids in the absorption image of the whole cell.

195

196 **2 Absorption Spectra of Eyespot (Figure 3)**

197 The bright-field microscopic image of the eyespot shows that various warm colors of yellow,
198 orange, and pale red are distributed variously in the eyespot. Depending on slight changes in the
199 depth of focus, the colors of eyespot varied diversely. It is observed that the area near the
200 boundary of the eyespot is pale red and the interior of it shows yellow or orange (Figure 1). The
201 absorption spectra near the center of the eyespot has a broad absorption maximum in the region
202 of 420 to 510 nm, which are consistent with the literature (James *et al.*, 1992; Jerome, 2012).

203 (a) E is an absorption spectrum of the chloroplast adjacent to the eyespot which has an
204 absorption peaks derived from Chlorophyll *a* (Chl-*a*) at 436 and 676 nm and a peak derived from
205 carotenoids at 488 nm. G is a chloroplast spectra existing at a location distant from the eyespot
206 and has a spectrum resembling the spectrum of E and each absorption peak is at about the same
207 wavelength. G has a higher absorbance at the absorption peak of Chl-*a*, which suggests that G
208 has constituents of chloroplasts present at higher density than E. In addition, comparing the
209 increase ratio of absorbance at the absorption peak of carotenoids with the Chl-*a* of G against E,
210 the ratio of increase was larger for the carotenoids. The ratio of increase in absorbance in the
211 wavelength other than the periphery of the absorption peak was also larger than that of Chl-*a*.
212 Particularly, from 600 nm to 520 nm, the absorbance of the spectrum of E decreases toward
213 shorter wavelengths, but the spectrum is nearly flat in the region corresponding to it. This
214 suggests that the presence of accessory pigment (carotenoids) is greater in places where
215 chloroplasts are dense, and that the light harvesting system is functioning more efficiently. For
216 carotenoids, it is suggested that G has a higher density of carotenoids by comparing the

217 absorption maximum at 488 nm. F shows the absorption spectrum near the border of the
218 chloroplast dense area, which has a single absorption peak characteristic at 405 nm.

219 (b) The spectrum of the outline of the eyespot is shown. Unlike the general spectrum of the
220 eyespot, the spectrum in the region A1 to A7 has a single absorption maximum at 516 nm.
221 Corresponding to the bright-field microscopic image, it shows that this region is pale red. On the
222 other hand, since the spectrum in the region from A8 to A9 shows a typical spectrum of the
223 eyespot, it is suggested that the composition of eyespot's pigments is changed greatly with the
224 boundary between A7 and A8 as the border. Among the carotenoids contained in the eyespot of
225 *E. gracilis*, canthaxanthin (467) and echinenone (458) are known to have a single absorption
226 maximum (Numbers in parentheses indicate wavelengths in diethyl ether (*Heelis et al., 1979*)).
227 Although the absorption spectrum of the pigments extracted from purple cabbage at pH 3.2 most
228 closely agrees with the spectrum and the color, a report that the eyespot contains anthocyanin has
229 not been found. (cf. The pH of the culture solution in this experiment is 3.5.)

230 (c) From the boundary of the eyespot toward the center, the absorption maximum wavelength
231 of the spectra similar to (b, A1 to A7) gradually shift to a shorter wavelength, and the shapes of
232 the maxima becomes broader. By correspondence with the bright-field microscopic image, it is
233 indicated that the vicinity of the boundary of the eyespot is pale red and the vicinity of the center
234 is yellow. Therefore, it is suggested that the spectrum having this single absorption maximum is a
235 pigment with pale red. In addition, since each slope on the longer wavelength side of the
236 maximum of the spectrum (B1 to B8) is smoothly connected to each other, this pigment was
237 suggested to be related to the main carotenoids constituting the eyespot.

238 (d) The data shows the spectra of a typical eyespot. This shows that the absorption decreases
239 from the center of the eyespot towards the boundary while the shapes of the spectra remains
240 almost the same.

241 (e), (f) In the vicinity of the center of the eyespot, a typical absorption spectra of the eyespot
242 are shown, but in the region of 410 to 540 nm, the absorbance of the spectrum of (e) increases
243 toward longer wavelengths and that of (f) decreases toward longer wavelengths.

244 (g), (h) The data shows that Chl-*a* is present in these regions since all the spectra have peaks at
245 about 676 nm. Since the characteristic absorption of carotenoids is shown in the spectra of D3 to
246 D8, it is suggested that a greater amount of carotenoids is contained than that contained in
247 chloroplasts. In the region of D9 to D13, it is considered that the carotenoids are contained in a
248 slightly larger amount than that contained in the chloroplast. This is because in these spectra the
249 absorption maximum of carotenoids at 490 nm is large relative to that of the carotenoid free
250 spectrum (D22). These graphs show that as a result of the absorption of carotenoids, the
251 absorbance of the spectra increase toward shorter wavelengths. However, since it does not show
252 the shapes of the spectra overlapping with the spectra of the typical eyespot, there may be
253 carotenoids of a different type from eyespot, or in a different form.

254 255 **3 Absorption Spectra of Hematochrome-like Granule (Figure 4)**

256 The absorption spectrum obtained when hematochrome is observed with the focus on the
257 coloring of warm color like eyespot has a basic structure like the Chl-*a* spectrum with an
258 additional characteristic peak at 620 nm. Every time the same hematochrome is measured,

259 different spectra are obtained. They generally show spectra with (C 10, C 11, D 9, D 10, etc) in
260 Figures (e)~(l).

261 Since the hematochrome which is observed is located in the region without chloroplasts, it is
262 considered that there is no contribution by absorption of Chl-*a*. In addition, although
263 hematochrome does not necessarily appear in a specific area, the hematochrome of present
264 observation is located near the eyespot, so that it was adopted for easy comparison with the
265 eyespot (Figure 2. (a), (c)).

266 (a) The data shows typical absorption spectrum of carotenoids contained in the eyespot.
267 Therefore, the absorption region in the vicinity is the eyespot. (Figure 2. (B)).

268
269 (b) The data shows the absorption spectrum in the region slightly away from the
270 hematochrome. This shows the same spectrum as the region exhibiting vivid green color in the
271 vicinity of the eyespot (Figure 3. (A). E).

272 (c) The data shows the absorption spectra of the boundary of hematochrome. They are spectra
273 similar to Chl-*a* and have an absorbance offset over the entire wavelength range, which is
274 consistent with showing dark green color in bright-field microscopic image.

275 (d) The data shows the spectra showing the dark green regions at the hematochrome boundary.
276 They have clearer minor peaks at 490, 580, 625, and 715 nm in addition to the major peaks at 676
277 nm and 440 nm characteristic of the absorption spectrum of Chl-*a* compared to (e). Therefore,
278 they are clearly different spectra from the absorption spectrum of the chloroplast.

279 (f) The data show that the absorbance above 730 nm for the absorption peak at 676 nm
280 increases from the center of hematochrome toward the boundary. The largest spectral change was
281 observed between the C12 and C13. This is considered to correspond to the boundary between
282 the dark red (C12) and dark green (C13) regions of the bright field observation image (Figure 2.
283 (A), (c)).

284 (k) The spectra show that the absorbance of hematochrome at 620 nm increases from the
285 boundary to the center (F1 to F3). However, the absorbance at 620 nm stops increasing at a
286 certain value (Absorbance = 0.17), whereas the absorbance increases at the range of 400 to 600
287 nm and 650 to 730 nm (F4 to F12). As a result, since the absorbance in the region of 580 to 650
288 nm and 730 nm or more becomes relatively small, it is expected to exhibit warm color. In fact,
289 the bright-field microscopic image of hematochrome in this region shows that it is warm color.
290 Spectra (Figures i, j, l) in the peripheral region of F1 to F10 also exhibit absorption spectra
291 similar to them. The fact that the absorbance in the entire spectrum shifts largely upward towards
292 the center of hematochrome and that the difference between the absorbance at 620 nm and 676
293 nm decreases is consistent with the fact that this region is dark red in bright-field microscopic
294 image. On the other hand, the spectrum in Fig. (k) has a small upward shift and the absorbance at
295 600 to 650 nm is small, suggesting that it shows a bright warm color.

296
297 (m), (n) Spectra with the shape similar to the absorption spectrum of the chloroplast was
298 obtained. This suggests that there are chloroplasts nearby, so influenced by them.

299

300 Discussion

301 In the eyespot and hematochrome, various absorption spectra were obtained depending on the
302 location, while almost the same spectra are obtained in the green region of *E. gracilis* where the
303 chloroplast exists. These results indicate that the eyespot and the hematochrome are characteristic
304 intracellular structures recognizable by microspectrophotometry. In particular, since
305 hematochrome resembles an eyespot in appearance and its absorption spectrum resembles a
306 chloroplast, so that attention must be paid when measuring the absorption by
307 microspectrophotometry of the eyespot where chloroplasts are present in the surroundings.
308 Actually, there is a report that seems to mistake a hematochrome for the eyespot, and the
309 spectrum of the eyespot indicated in that report was very similar to the spectrum of
310 hematochrome in the study (Werner *et al*, 1990).

311 There is also a report that various spectra were obtained for each measurement at the same
312 eyespot by microspectrophotometry (Jerome, 2012). This was considered to be caused by the
313 change in the focus at every measurement and the change in the position and distribution of the
314 carotenoid granules contained in the eyespot everytime the cell shape deforms by the euglena
315 movement, since the granules are not composed of a rigid structure (Benedetti *et al.*, 1976) and
316 are irregular sequences and the granules are cytoplasmic side organelles bound to the cell
317 membrane (Kivic & Vesk, 1972).

318 It is considered to be difficult to identify each carotenoid constituting the eyespot from the
319 spectra of the eyespot obtained by microspectrophotometry because the absorption bands of each
320 carotenoid are almost the same (Jerome, 2012). There are two reports that carotenoids contained
321 in the eyespot or in the whole cells of *E. gracilis* were chemically analyzed. Each showed
322 different types of carotenoids and their content ratios (Norman & Timothy, 1960; Heelis *et al.*,
323 1979). Although we could not identify carotenoids contained in each intracellular structure in this
324 study, we could confirm the presence or absence of pigments with characteristic spectra.

325 Although the origin of hematochrome has not yet been elucidated, there is a hypothesis that its
326 origin is an eyespot (Jerome, 2012). But the absorption spectra in the regions where the absorption
327 of the hematochrome is large have an absorption peak at 676 nm characteristic to Chl-*a*, suggesting
328 that its origin may be chloroplast. In addition, many spectra of hematochrome obtained had large
329 absorption in the absorption band of carotenoids although there is a report that hematochrome does
330 not contain carotenoids (Britton & Goodwin, 2013). If this is true, it is necessary to exclude the
331 region of hematochrome when analyzing the absorption image of carotenoids contained in the
332 whole cells, because the absorption of hematochrome is large at 488 nm which is the absorption
333 maximum of the carotenoids (Figure 2. (C)). However, since the chloroplast contains carotenoids,
334 this study alone cannot prove the hypothesis that the origin is chloroplast. Therefore, it is suggested
335 that another approach such as chemical analysis targeting only hematochrome is required as a
336 future task.

337

338 **Conclusion and Prospects**

339 The present measurement method enabled us to simultaneously and comprehensively obtain
340 absorbance information of various microscopic regions of an organelle in a single measurement.
341 By contrast, the conventional methods allow the cell to move or the pigments to bleach owing to a
342 long measurement time.

343 The absorption spectrum of hematochrome of *E. gracilis* showed a distinctly different shape
344 from the spectrum of the eyespot, characterized by a peak at 620 nm and that at 676 nm coinciding
345 with the absorption peak of Chl-*a*. This indicates that hematochrome is an organelle composed of
346 a pigment different from the eyespot. This distinction made it clear that this technique can be used
347 for fundamental research on intracellular structural analysis and applied research for screening of
348 carotenoids-rich competent cells.

349 As a next step, we would like to pursue the conditions to grow the cells which contain more
350 carotenoids by selecting such cells to have the higher maximum absorbance values of carotenoids
351 than the average: The average is determined from the distribution of the maximum carotenoids'
352 absorbance of individual cells, which is extracted from the absorbance spectral image of each
353 whole cell excluding the regions occupied by hematochromes.

354
355 **Acknowledgments:** The authors would like to thank Research Center for Green and Safety
356 Sciences, Tokyo University of Science for financial support.

357
358 **Author Contributions:** K.Yamashita. and E.T. conceived and designed the experiments;
359 K.Yamashita prepared samples and performed the experiments; T.Y. and M.H. contributed the
360 experiments. Y.N. made the data analysis program. K.Yamada and K.S. contributed sample
361 preparation; E.T. designed the measurement system. T.I. contributed buildup of the system.
362 K.Yamashita and E.T. wrote the paper.

363 **Conflicts of Interest:** The authors declare no conflict of interest.

364 References

365 **Barbara Demmig-Adams. 1990.** Carotenoids and photoprotection in plants: a role for the
366 xanthophyll zeaxanthin. *Biochim Biophys Acta.* **1020**:1–24 DOI 10.1016/0005-
367 2728(90)90088-L.

368 **Barsanti L, Coltelli P, Evangelista V, Passarelli V, Frassanito AM, Vesentini N, Santoro F,**
369 **Gualtieri P. 2009.** In vivo absorption spectra of the two stable states of the *Euglena*
370 photoreceptor photocycle. *Photochem Photobiol* **85**:304-312 DOI 10.1111/j.1751-
371 1097.2008.00438.x.

372 **Benedetti PA, Bianchini G, Checcucci A, Ferrara R, Grassi S. 1976.** Spectroscopic
373 properties and related functions of the stigma measured in living cells of *Euglena gracilis*.
374 *Arch. Microbiol.* **111**:73-76 DOI 10.1007/BF00446551.

375 **Benedetti PA, Bianchini G, Checcucci A, Ferrara R, Grassi S. 1976.** Spectroscopic properties
376 and related functions of the stigma measured in living cells of *Euglena gracilis*. *Arch*
377 *Microbiol.* **111**:73-76 DOI 10.1007/BF00446551.

378 **Cramer M, Myers J. 1952.** Growth and photosynthetic characteristics of *euglena gracilis*.
379 *Archiv für Mikrobiologie* **17**:384-402 DOI 10.1007/BF00410835.

380 **Delia B, Rodriguez-Amaya. 2015.** Food Carotenoids: Chemistry, Biology and
381 Technology. *Wiley-Blackwell* DOI 10.1002/9781118864364.

- 382 **Dennis E Buetow 1982.** The Biology of *Euglena*: Physiology. Academic Press.
- 383 **G Britton,TW Goodwin. 2013.** Carotenoid Chemistry and Biochemistry: Proceedings of the 6th
384 International Symposium on Carotenoids. *Pergamon*.
- 385 **Georg Kreimer. 2009.** The green algal eyespot apparatus: a primordial visual system and more?
386 *Current Genetics* **55**:19–43 DOI 10.1007/s00294-008-0224-8.
- 387 **GK STROTHER, JJ WOLKEN. 1961.** In vivo Absorption Spectra of *Euglena*: Ghloroplast and
388 Eyespot. *J. PROTOZOOL.* **8**:261-265 DOI 10.1111/j.1550-7408.1961.tb01213.x.
- 389 **Gordon HT, Bauernfeind JC. 1982.** Carotenoids as food colorants. *Crit Rev Food Sci Nutr.*
390 **18**:59-97 DOI 10.1080/10408398209527357.
- 391 **Hardeep S Tuli, Prachi Chaudhary, Vikas Beniwal, Anil K Sharma. 2015.** Microbial
392 pigments as natural color sources: current trends and future perspectives. *J Food Sci Technol.*
393 **52**:4669–4678 DOI 10.1007/s13197-014-1601-6.
- 394 **Hashimoto H, Uragami C, Cogdell RJ.2016.** Carotenoids and Photosynthesis. Springer
395 DOI10.1007/978-3-319-39126-7_4.
- 396 **Havaux M. 1998.** Carotenoids as membrane stabilizers in chloroplasts. *Trends Plant Sci.* **3**:147–
397 151 DOI 10.1016/S1360-1385(98)01200-X.
- 398 **Heelis DV, Kernick W, Phillips GO, Davies K. 1979.** Separation and identification of the
399 carotenoid pigments of stigmata isolated from light-grown cells of *Euglena gracilis* strain Z.
400 *Arch Microbiol.* **121**:207-11 DOI 10.1007/BF00425057.
- 401 **Inui H, Miyatake K, Nakano Y, Kitaoka S. 1982.** Wax ester fermentation in *Euglena gracilis*.
402 *FEBS Lett.* **150**:89–93 DOI 10.1016/0014-5793(82)81310-0.
- 403 **Isono T, Yamashita K, Momose D, Kobayashi H, Kitamura M, Nishiyama Y. Hosoya T,**
404 **Kanda H, Kudo A, Okada N, Yagi T, Nakata K, Mineki S, Tokunaga E. 2015.** Scan-Free
405 Absorbance Spectral Imaging $A(x, y, \lambda)$ of Single Live Algal Cells for Quantifying Absorbance
406 of Cell Suspensions. *PLoS ONE* **10** DOI 10.1371/journal.pone.0128002.
- 407 **Iwata O, Yamada K, Ito T, Ozeki Y, Suzuki K, Goda K. 2017.** Technology for Developing
408 Super Microalgal Biofuels. *Seibutsu Butsuri* DOI 10.2142/biophys.57.235.
- 409 **James TW, Crescitelli F, Loew ER, McFarland WN. 1992.** The eyespot of *Euglena gracilis*: a
410 microspectrophotometric study. *Vision Res* **32**:1583-1591 DOI 10.1016/0042-6989(92)90151-
411 8.
- 412 **Jerome J Wolken. 2013.** Invertebrate Photoreceptors: A Comparative Analysis. *Academic Press*.
- 413 **Jerome J, Wolken. 2012.** *Euglena*: An Experimental Organism for Biochemical and Biophysical
414 Studies. *Springer Science & Business Media*.

- 415 **Joanna Fiedor, Květoslava Burda. 2014.** Potential Role of Carotenoids as Antioxidants in
416 Human Health and Disease. *Nutrients*. **6**:466-488 DOI 10.3390/nu6020466.
- 417 **Johnson EJ. 2002.** The role of carotenoids in human health. *Nutr Clin Care*. **5**:56-65 DOI
418 10.1046/j.1523-5408.2002.00004.x.
- 419 **Kato S, Soshino M, Takaichi S, Ishikawa T, Nagata N, Asahina M, Shinomura T. 2017.**
420 Suppression of the phytoene synthase gene (*Egcr1B*) alters carotenoid content and intracellular
421 structure of *Euglena gracilis*. *BMC Plant Biol*. **17**:125 DOI 10.1186/s12870-017-1066-7.
- 422 **Kivic PA, Vesik M. 1972.** Structure and function in the euglenoid eyespot apparatus: The fine
423 structure, and response to environmental changes. *Planta*. **105**:1-14 DOI
424 doi.org/10.1007/BF00385158.
- 425 **Koren LE, Hutner SH. 1967.** High-yield media for photosynthesizing *Euglena gracilis* Z. *J.*
426 *Protozool*. **14**.
- 427 **Lee JY, Clarke ML, Tokumasu F, Lesoine JF, Allen DW, Chang R, et al. 2012.** Absorption-
428 Based Hyperspectral Imaging and Analysis of Single Erythrocytes. *IEEE J. Selected Topics in*
429 *Quantum Electronics* **18**:1130–1139 DOI 10.1109/JSTQE.2011.2164239.
- 430 **Matsuoka H, Kosai Y, Saito M, Takeyama N, Suto H. 2002.** Single-cell viability assessment
431 with a novel spectro-imaging system. *J. Biotechnol*. **94**:299–308 DOI 10.1016/S0168-
432 1656(01)00431-X.
- 433 **Maxim E Darwin, Wolfram Sterry, Juergen Lademann, Theognosia Vergou. 2011.** The Role
434 of Carotenoids in Human Skin. *Molecules* **16**:10491-10506 DOI
435 10.3390/molecules161210491.
- 436 **Merete Grung, Georg Kreimer, Michael Calenberg, Michael Melkonian, Synnøve Liaen-**
437 **Jensen. 1994.** Carotenoids in the eyespot apparatus of the flagellate green alga *Spermatozopsis*
438 *similis*: Adaptation to the retinal-based photoreceptor. *Planta* **193**:38-43 DOI
439 10.1007/BF00191604.
- 440 **Mineo Iseki. 2007.** Molecular mechanism of light sensing in *Euglena*. *Jpn. J. Protozool*. **40**:93-
441 100.
- 442 **N Hagen, MW Kudenov. 2013.** Review of snapshot spectral imaging Technologies. *Opt. Eng.*
443 **52** DOI 10.1117/1.OE.52.9.090901.
- 444 **N Hagen, RT Kester, L Gao, TS Tkaczy. 2012.** Snapshot advantage: a review of the light
445 collection improvement for parallel high-dimensional measurement systems. *Opt. Eng.* **51** DOI
446 10.1117/1.OE.51.11.111702.
- 447 **Norman I Krinsky, Timothy H Goldsmith. 1960.** The carotenoids of the flagellated
448 alga, *Euglena gracilis*. *Archives of Biochemistry and Biophysics* **91**:271-279 DOI
449 10.1016/0003-9861(60)90501-4.

- 450 **Ozasa K, Jeesoo Lee, Simon Song, Maeda M. 2014.** Transient Freezing Behavior in
451 Photophobic Responses of *Euglena gracilis* investigated in a Microfluidic Device. *Plant and*
452 *Cell Physiology*. **55**:1704-1712 DOI 10.1093/pcp/pcu101.
- 453 **RT Kester, N Bedard, L Gao, TS Tkaczyk. 2011.** Real-time snapshot hyperspectral imaging
454 endoscope. *J. Biomed. Opt.* **16** DOI 10.1117/1.3574756.
- 455 **Steven D. Schwartzbach, Shigeoka S. 2017.** *Euglena*: Biochemistry, Cell and Molecular
456 Biology. *Springer*.
- 457 **Sugiyama A, Suzuki K, Mitra S, Arashida R, Yoshida E, Nakano R, Yabuta Y, Takeuchi T.**
458 **2009.** Hepatoprotective effects of paramylon, a beta-1, 3-D-glucan isolated from *Euglena*
459 *gracilis* Z, on acute liver injury induced by carbon tetrachloride in rats. *J. Vet. Med. Sci.*
460 **71**:885–890 DOI 10.1292/jvms.71.885.
- 461 **Suzuki K. 2017.** Large-Scale Cultivation of *Euglena*. *Adv Exp Med Biol*. **979**:285-293 DOI
462 10.1007/978-3-319-54910-1_14.
- 463 **Takaichi S, Mimuro M, Tomita Y.2006.** Carotenoids - its diversity and its physiological activity.
464 *Shokabo*.
- 465 **Takeyama H, Kanamaru A, Yoshino Y, Kakuta H, Kawamura Y, Matsunaga T. 1997.**
466 Production of antioxidant vitamins, β -carotene, vitamin C, and vitamin E, by two-step culture
467 of *Euglena gracilis* Z. *Biotechnology and Bioengineering* **53**: 185-190 DOI
468 10.1002/(SICI)1097-0290(19970120)53:2<185::AID-BIT8>3.0.CO;2-K.
- 469 **Valter Evangelista, Mauro Evangelisti, Laura Barsanti, Anna Maria Frassanito, Vincenzo**
470 **Passarelli, Paolo Gualtieri. 2007.** A polychromator-based microspectrophotometer. *Int J Biol*
471 *Sci* **3**:251-256 DOI 10.7150/ijbs.3.251.
- 472 **Wakisaka Y, Suzuki Y, Iwata O, Nakashima A, Ito T, Hirose M, Domon R, Sugawara M,**
473 **Tsumura N, Watarai H, Shimobaba T, Suzuki K, Goda K, Ozeki Y. 2016.** Probing the
474 metabolic heterogeneity of live *Euglena gracilis* with stimulated Raman scattering microscopy.
475 *Nat. Microbiol.* **1** DOI 10.1038/nmicrobiol.2016.124.
- 476 **Werner Schmidt, Paul Galland, Horst Senger, Furuya M. 1990.** Microspectrophotometry of
477 *Euglena gracilis* Pterin- and flavin-like fluorescence in the paraflagellar body Pterin- and
478 flavin-like fluorescence in the paraflagellar body. *Planta* **182**:375-381 DOI
479 10.1007/BF02411388.
- 480 **Wojcik K, Dobrucki J W. 2008.** Interaction of a DNA intercalator DRAQ5, and a minor groove
481 binder SYTO17, with chromatin in live cells-influence on chromatin organization and histone-
482 DNA interactions. *Cytometry A* **73a**:555–562 DOI 10.1002/cyto.a.20573.
- 483 **Yamada K, Suzuki H, Takeuchi T, Kazama Y, Mitra S, Abe T, Goda K, Suzuki K, Iwata O.**
484 **2016a.** Efficient selective breeding of live oil-rich *Euglena gracilis* with fluorescence-activated
485 cell sorting. *Scientific Reports* **6** DOI 10.1038/srep26327.

- 486 **Yamada K, Kazama Y, Mitra S, Marukawa Y, Arashida R, Abe T, Ishikawa T, Suzuki K.**
487 **2016b.** Production of a thermal stress resistant mutant *Euglena gracilis* strain using Fe-ion
488 beam irradiation. *Biosci Biotechnol Biochem.* **80**:1650-1656 DOI
489 10.1080/09168451.2016.1171702.
- 490 **Yamaji Nakano. 1980.** Chloroplast Replication in *Euglena gracilis* Grown in Cadmium-Ion
491 Containing Media. *Agric. Biol. Chem.* **44**:2733-2734 DOI 10.1080/00021369.1980.10864396.

Figure 1

(a) A bright-field microscopic image of *E. gracilis*. (b) Enlarged view near the eyespot. (c) The colors of the eyespot and hematochrome-like granule are changed as the depth of focus is slightly changed.

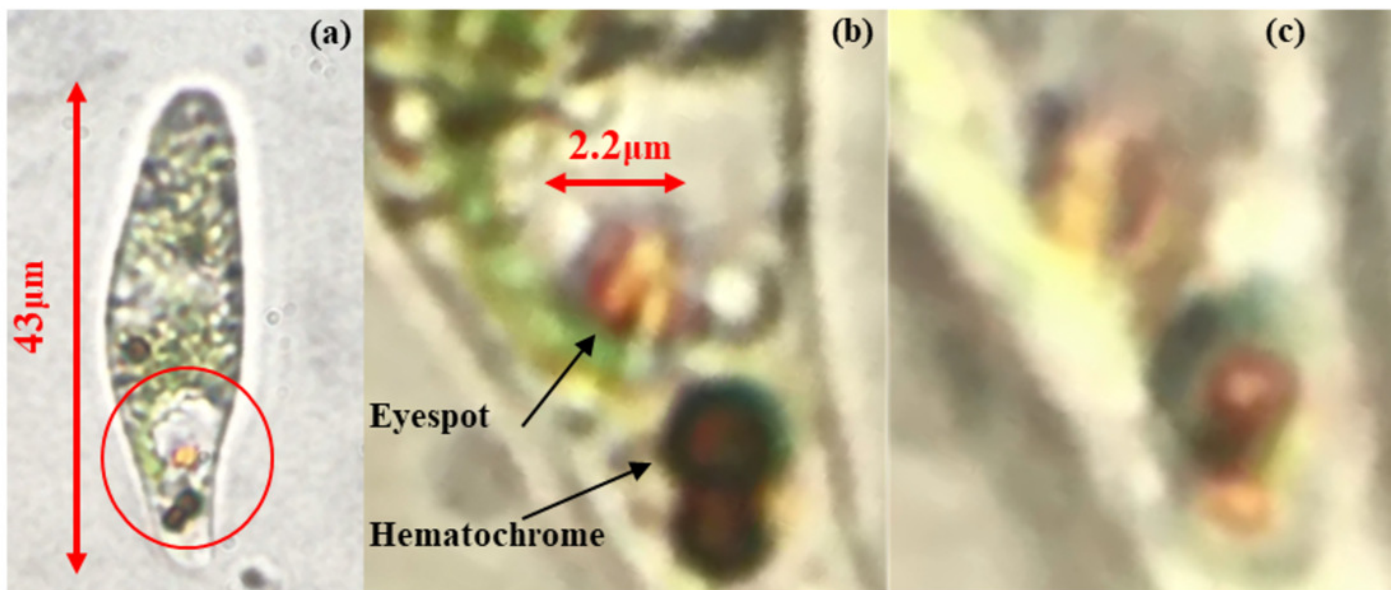


Figure 2

(a) A bright-field microscopic image of *E. gracilis*. (b) Absorption image (at 488 nm) inside the eyespot and in the surrounding area. (c) Absorption image (at 488 nm) inside the hematochrome-like granule and in the surrounding area. Du

Note: The absorption maximum wavelength of carotenoid is assumed to be 488 nm.

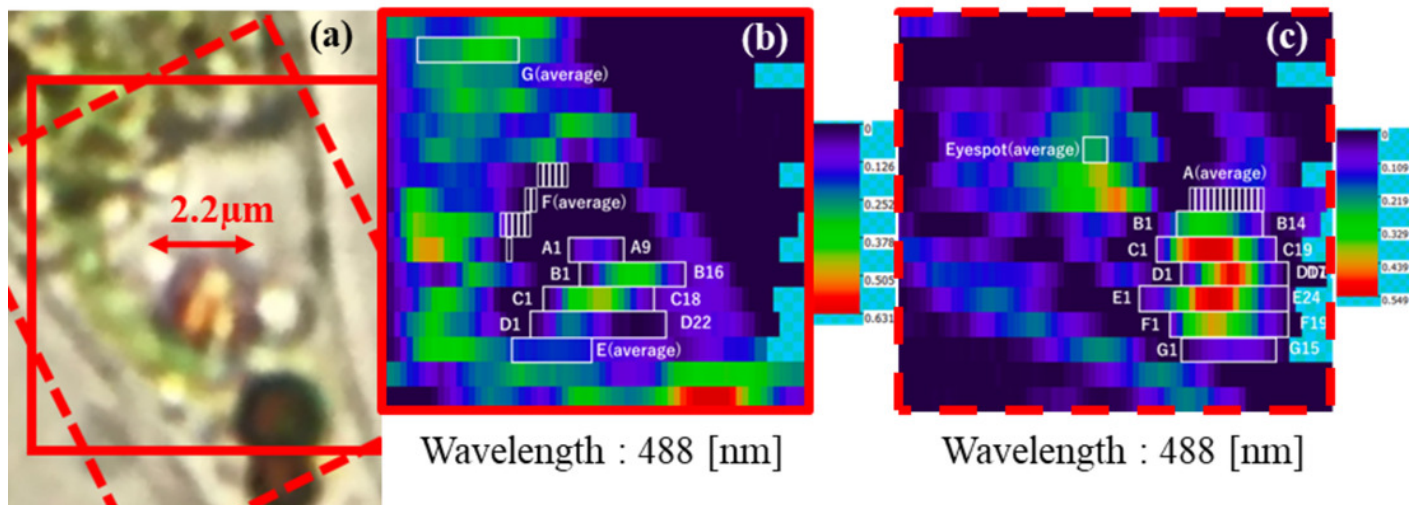


Figure 3

.Absorption spectra of the eyespot of *E. gracilis*.

(Each spectrum corresponds to the labeled position in Figure 2. (b).)

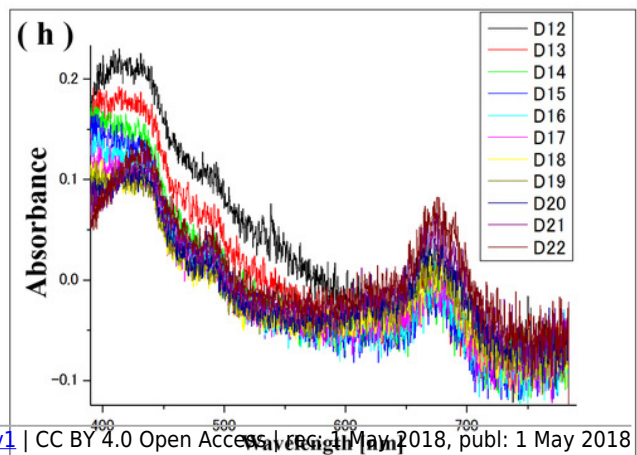
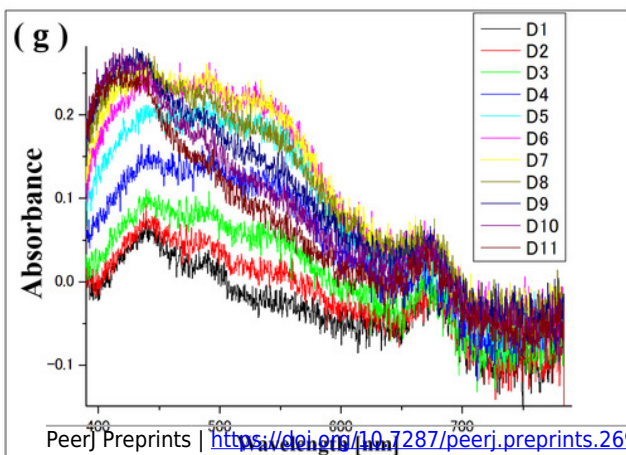
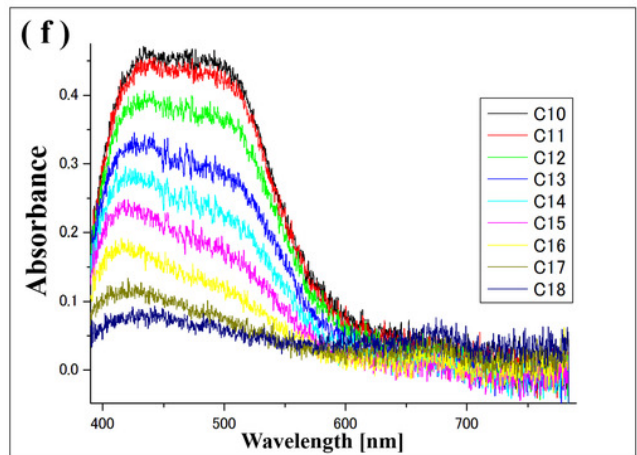
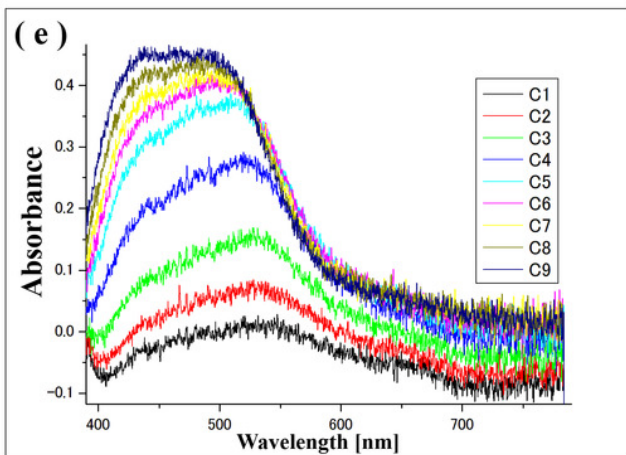
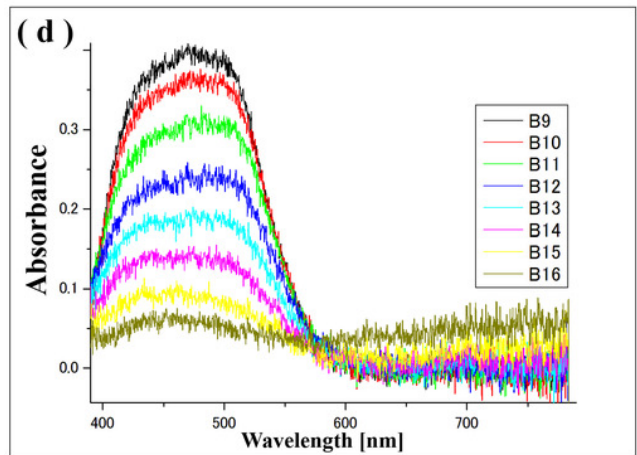
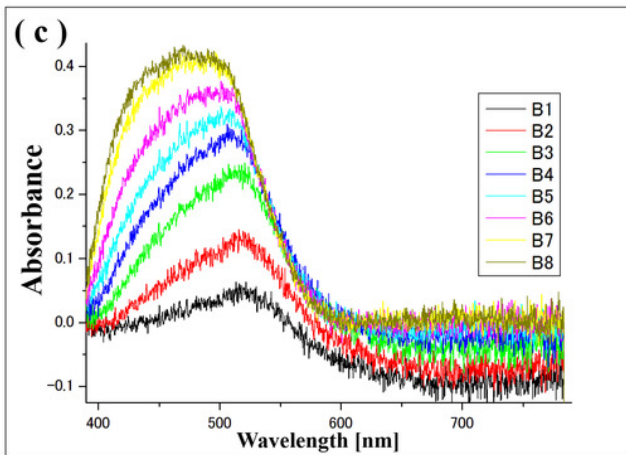
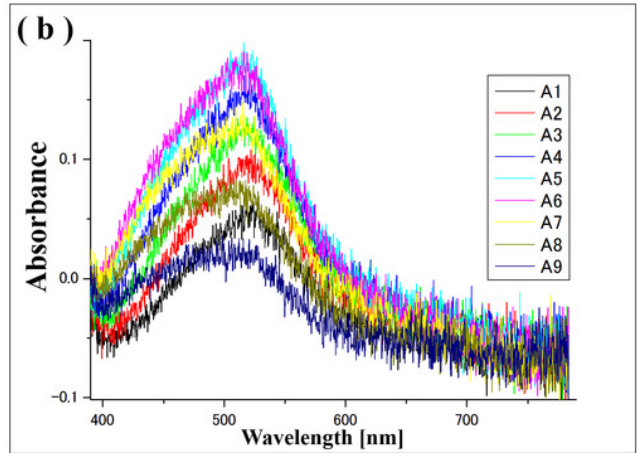
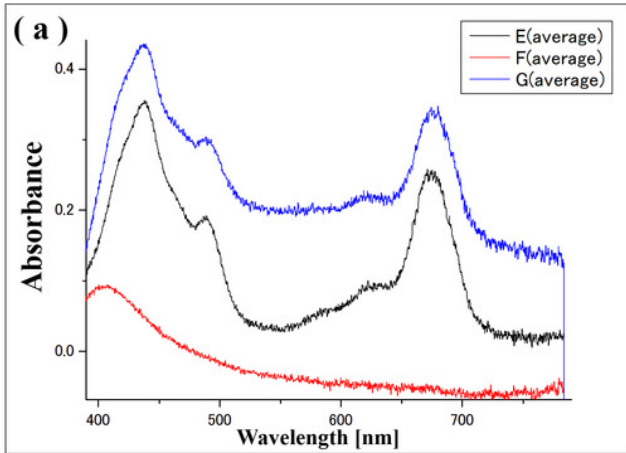


Figure 4

Absorption spectra of the hematochrome-like granule of *E. gracilis*.

(Each spectrum corresponds to the labeled position in Figure 2. (c).)

